

# Enhanced Brain MRI disease classification via wavelet decomposition-infused CNN architecture featuring residual blocks

J.L. Mudegaonkar<sup>1</sup>, D.M. Yadav<sup>2</sup>

<sup>1</sup>GH Raison College of Engineering and Management, Wagholi, Pune, India, <sup>2</sup>SND College of Engineering and Research Centre, Yeola, Nashik, India

Received on: 03-Mar-2024, Accepted and Published on: 10-09-2024

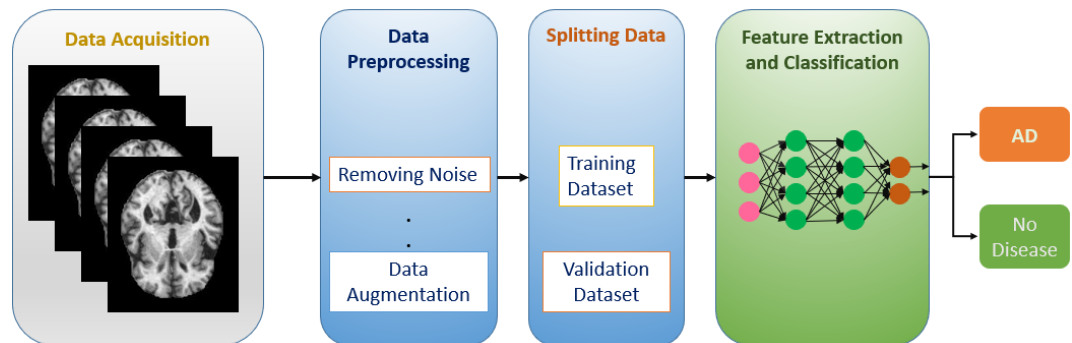
Article

## ABSTRACT

Precisely identifying diseases from brain Magnetic Resonance Imaging (MRI) plays a pivotal role in both diagnosing medical conditions and formulating effective treatment plans although it faces challenges owing to the complexity of the brain. Recent studies highlight

CNNs' efficacy in disease classification. We propose a CNN model integrating wavelet decomposition and Residual blocks to classify Alzheimer's disease, brain tumors, and normal conditions from MRI scans. Four stages of wavelet decomposition extract features, aiding Residual blocks in efficient deep network training. Evaluation on MRI datasets show high accuracy, specificity, and sensitivity (0.945, 0.985, and 0.945 respectively), surpassing existing models. This model enhances diagnosis and treatment planning efficiency. Exploring various wavelet types, Daubechies-9 (DB9) wavelet proves superior, emphasizing wavelet selection importance. The model excels in binary, three-way, and four-way classifications, showcasing its adaptability and potential in brain MRI analysis

**Keywords:** Disease Detection, Brain MRI, CNN Model, Wavelet Decomposition, Residual Blocks



## INTRODUCTION

Magnetic Resonance Imaging (MRI) plays a pivotal role in both diagnosing medical conditions and formulating effective treatment plans for cancer, Alzheimer's, and cardiovascular conditions. It offers a non-invasive means of capturing highly detailed images of internal organs and tissues, so it becomes essential tool for disease detection and diagnosis.<sup>1</sup> However, manual interpretation of MRI images by radiologists for dealing with multiple diseases in a single patient becomes time-consuming, subjective, and prone to errors<sup>2</sup>, thus, the need arises to develop automated methods for disease detection and diagnosis from MRI images.

Deep learning, which is a part of artificial intelligence, is really promising in analyzing MRI scans, especially for finding and diagnosing diseases.<sup>3</sup> Disease classification is performed by deep learning models that learn complex representations of MRI and automatically extract relevant features. Deep learning models detect single diseases in MRI images; research on detecting multiple diseases in MRI is limited.<sup>4</sup>

Deep learning-based multiple brain disease detection from MRI is an important application of artificial intelligence in healthcare.<sup>5</sup> MRI is a helpful way to scan brain internal structure without surgery. It gives clear pictures of how the brain looks and works. This technology aids doctors in diagnosing various brain diseases, including Alzheimer's, multiple sclerosis, Parkinson's, stroke and brain tumors, facilitating timely and accurate treatment interventions.

Deep learning algorithms trained on MRI datasets enhance multiple brain disease detection<sup>6</sup>, improving diagnosis and treatment outcomes. This approach overcomes challenges like inter-observer variability<sup>7</sup>, streamlining diagnosis and resource use.

\*Corresponding Author: J.L. Mudegaonkar  
Tel: +91-9421090805; Email: jagdishmudegaonkar@gmail.com,

Cite as: J. Integr. Sci. Technol., 2025, 13(1), 1005.  
URN:NBN:sciencein.jist.2025.v13.1005  
DOI: 10.62110/sciencein.jist.2025.v13.1005



©Authors CC4-NC-ND, ScienceIN  
http://pubs.thesciencein.org/jist

It promises to revolutionize brain disease management, improving patient care, cutting costs, and advancing medical research.<sup>8</sup>

Images produced from a 1.5 Tesla MRI scanner are often called "1.5T images". A commonly employed field strength in clinical practice, this technique excels in producing high-quality brain images without any compromise on the accuracy of the results. These images show great potential for MRI processing for multiple brain disease detection due to several reasons:

**High Signal-to-Noise Ratio (SNR):** The high SNR of 1.5T MRI images facilitates easy identification of subtle brain changes, which may indicate various brain diseases, owing to their strong contrast and detail.<sup>9</sup>

**Improved Spatial Resolution:** 1.5T MRI images have improved spatial resolution compared to lower field strengths, allowing for better visualization of small anatomical structures and lesions in the brain.<sup>9</sup>

**Standardization:** 1.5T MRI scanners are widely used in clinical practice, and there is a significant amount of data available in the form of large databases of MRI images.<sup>9</sup> Large datasets enhance deep learning for accurate, reliable detection of multiple brain diseases.

**Non-invasive:** MRI is non-invasive, meaning it doesn't involve cuts or injections, lowering the chances of complications linked with invasive methods.

Overall, 1.5T MRI images show great potential for MRI processing for multiple brain disease detection due to their high SNR, improved spatial resolution, standardization, and non-invasiveness. By employing deep learning algorithms trained on large sets of 1.5T MRI images, we can improve the accuracy and speed of detecting different brain diseases. so, MRI technology has the potential to significantly improve patient outcomes and contribute to a more efficient healthcare system.

In brain MRI image analysis for multi disease classification task, disease based relevant features are important to be captured. The appearance of brain MRI as per diseases can be understood from the MRI images shown in Figure1.

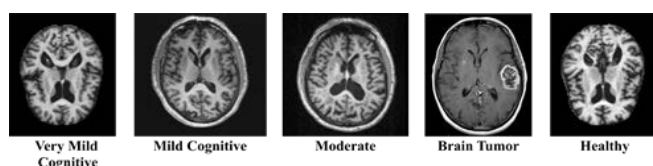


**Figure 1:** Brain MRI for different Diseases

This paper has made significant strides in magnetic resonance imaging analysis for disease detection and diagnosis. Summary of the key contributions is as follows

**Innovative Model Fusion:** We introduced a cutting-edge approach by fusing wavelet features with Residual Blocks in a Convolutional Neural Network (CNN). This novel fusion technique not only capitalizes on the strengths of both wavelet analysis and Residual Blocks but it also enables the extraction of selective relevant features from MRI data, thereby enhancing the precision of the classification process.

**Comprehensive Performance Assessment:** In this study accuracy, sensitivity, specificity, and F1-score are the evaluation

parameters, assessed to find out the effectiveness in disease detection.

This paper enhances disease detection from MRI images with augmented datasets and a novel CNN architecture, surpassing state-of-the-art models. It promises improved early diagnosis of Tumor and Alzheimer's diseases.

## RELATED WORK

Tolosa et al.<sup>10</sup> applied MRI image processing to detect Parkinson's disease, facing challenges from errors caused by other conditions. Specialized movement-disorder units improved diagnostic accuracy for parkinsonian syndromes. Danielyan et al.<sup>11</sup> highlighted neurological abnormalities, like dyskinesias and parkinsonian signs, in drug-naïve individuals. Islam et al.<sup>12</sup> highlighted the importance of MRI in diagnosing Alzheimer's disease and introduced a deep neural network as a proposed solution.

Fontana et al.<sup>13</sup> utilized EEG signal processing for Alzheimer's disease diagnosis, correlating with disease traits. Shatte et al.<sup>14</sup> surveyed machine learning's roles in brain disease detection, prognosis, public health, and research. Salvatore et al.<sup>15</sup> achieved detection of Progressive Supranuclear Palsy and Parkinson's disease using MRI data with accuracy over 90%.

Sorour et al.<sup>16</sup> classified MRI images into AD, MCI, or NC, comparing performance of neural networks. Mahmud et al.<sup>17</sup> used EEG acquisition for brain disease identification, outlining future research directions. Poldrack<sup>18</sup> studied Python's role in reproducible data analysis, leveraging software engineering advances. Mahmud<sup>19</sup> surveyed DL and RL applications in biological data mining, comparing performances across datasets. Mahmud et al.<sup>20</sup> explored DL architectures' applications to biological data, investigating open-access sources and tools. Basher et al.<sup>21</sup> constructed a CNN model for hippocampal volume prediction from MRI scans, using preprocessing. Lin et al.<sup>22</sup> processed MRI data for detection of Alzheimer's with high accuracy and AUC. Zou et al.<sup>23</sup> suggested using 3-D Convolutional Neural Networks (CNNs) based on deep learning for diagnosing psychiatric disorders. Feng et al.<sup>24</sup> derived deep features from MRI and PET, outperforming related algorithms in disease differentiation.

Jena et al.<sup>25</sup> investigated brain tumour segmentation using Fuzzy C Means method and various algorithms like SVM, decision tree, random forest, and K-nearest Neighbor are used as classifiers. The hand written material based Alzheimer's prediction approach is considered by Cilia et al.<sup>26</sup>. The method involves classification of images drawn by Alzheimer's patient and use of transfer learning approach of CNN. Alloui et al.<sup>27</sup> provided study of CNN based Alzheimer's detection from Brain MRI. The comparative of UNET with particle swarm optimized Fuzzy C-Means segmentation is provided. Kaur et al.<sup>28</sup> used different standard CNN models for retraining on Harvard clinical dataset. The Alzheimer detection AlexNet shown better performance among all.

Given the reviewed studies' focus on neuroimaging for disease detection, the development of a method combining Discrete Wavelet Transform (DWT) with residual-block based Convolutional Neural Networks (CNNs) is warranted. These studies, such as those by Tolosa et al.<sup>10</sup> and Danielyan et al.<sup>11</sup>, reveal

challenges in accurately detecting Parkinson's and neurological abnormalities. Islam et al.'s <sup>12</sup> emphasis on MRI's significance in Alzheimer's diagnosis supports the need for an improved approach. Additionally, Salvatore et al. <sup>15</sup> present a successful Parkinson's detection method, demonstrating the potential of advanced techniques. The DWT-residual CNN model we propose can overcome these challenges by combining wavelet transformation and deep learning. This approach improves accuracy in diagnosing neuroimaging-based diseases, in line with the latest advancements in the field.

## METHODOLOGY

In this study, the methodology comprises four stages, illustrated in the Block Diagram Representation of Stages of Proposed Work depicted in Figure 2.

The first stage involved dataset preparation, which included the collection and preprocessing of brain MRI images from standard public repositories. The collected datasets included Alzheimer's disease, brain tumor, and normal/healthy conditions MRI images. The second stage involved the composition of a customized CNN model using wavelet decomposition-based feature extraction and Residual blocks. The proposed model consists of four levels of wavelet decomposition and 17 Residual blocks. In the third stage, experimentation took place, which included selecting a suitable wavelet type for feature extraction. Additionally, the proposed model's performance was evaluated in binary, three-way, and four-way classification tasks. An evaluation of the model's effectiveness was conducted against several cutting edge models, including VggNet-16 <sup>29</sup>, ResNet-50 <sup>30</sup>, ResNet-101 <sup>30</sup>, DenseNet-121 <sup>31</sup>, Xception <sup>32</sup>, and MobileNet-V2 <sup>33</sup>. In the final stage, the experimental results were analyzed, showcasing the exceptional performance of the proposed CNN model in accurately classifying brain MRI images into multiple disease categories.

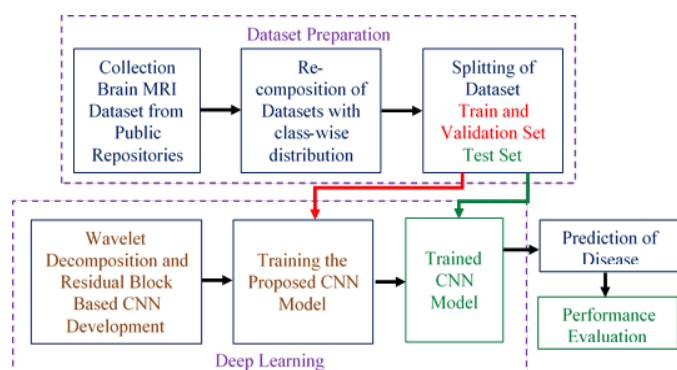


**Figure 2.** Block Diagram Representation of Stages of Proposed Work

**Dataset Preparation**

In this study, the dataset was acquired from kaggle: A standard public repository, as specified in Table 1. These repositories provided labeled datasets for the research. The Alzheimer's dataset from Kaggle was utilized, which consists of MRI images distributed across four classes, allowing for a four-way classification task. The Brain Tumor dataset was also used, containing MRI images for binary classification. Additionally, images from both datasets that depict normal/healthy conditions

were used for experimentation. To expand the dataset size, augmentation techniques were utilized, incorporating methods such as horizontal and vertical image flipping.

**Table 1:** Dataset obtained from standard public repositories

Dataset	Total Number of Images
Alzheimer Kaggle Dataset <sup>34</sup>	6400
Brain tumor dataset with Yes and No class	253
Brain Tumor dataset	200
Total	6853

The DB9 wavelet transform, derived from the Daubechies 9/7 wavelet function, is extensively utilized in signal processing, encompassing image and audio compression. Its popularity stems from its ability to localize frequencies effectively and preserve signal characteristics. It employs two filter pairs to split signals into scale-specific approximation and detail coefficients, achieved through convolutions and downsampling, recursively applied for desired decomposition levels.<sup>35</sup>

$h_0 =$	[0.03	-0.02	-0.08	0.27	0.60	0.27	-0.08	-0.02	0.03]
$h_1 =$	[-0.05	0.03	0.30	-0.56	0.30	0.03	-0.05	0.00	0.00]
$g_0 =$	[0.00	0.05	0.03	-0.30	-0.56	-0.30	0.03	0.05	0.00]
$g_1 =$	[0.00	0.00	-0.03	-0.02	0.08	0.27	-0.60	0.27	0.08]

Where, "h0" represents a low-pass filter and "h1" represents high-pass filters for decomposition, whereas "g0" denotes a low-pass filter and "g1" signifies high-pass filters for reconstruction.

Mathematically expression for DB9 wavelet transform is as follows:

Let,  $x[n]$  be the input signal, and let  $a_j[n]$  and  $d_j[n]$  be the approximation and detail coefficients at level  $j$ , respectively. The DB9 wavelet transform can be defined recursively as:

$$a_{j+1}[n] = (a_j * h_0)[2n] + (d_j * h_1)[2n] \quad d_{j+1}[n] = (a_j * g_0)[2n] + (d_j * g_1)[2n] \quad \dots(1)$$

Where  $*$  denotes the convolution operation,  $[2n]$  denotes downsampling by a factor of two, and  $a_0 = x$ .

**Residual Block:** Residual blocks are pivotal in convolutional neural networks (CNNs), initially proposed by He et al. in 2016 <sup>30</sup>. The structure of a residual is shown in Figure 3.

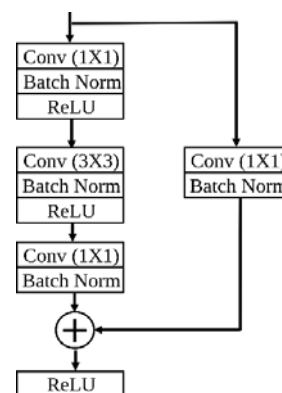


**Figure 3:** Residual Block

The Residual Block operates by first taking input data from the previous layer, then extracting key features through convolutional operations and applying activation functions to add non-linearity. Simultaneously, it retains a copy of the original input through a shortcut connection. The output of the convolutional layers is combined with this original input, creating a residual mapping that captures the difference between the input and output. Finally, the combined result is passed to the next layer. This approach enables more effective learning by facilitating gradient flow and aiding in the understanding of complex data patterns. When training highly complex networks, this technique is highly beneficial, as it can mitigate the vanishing gradient issue<sup>36</sup> that often arises when backpropagating through multiple layers. The mathematically a residual block is expressed as,

$$y = F(x) + x \quad \dots(2)$$

Given input  $x$ , residual function  $F$  is learned, yielding output  $y$ . Addition is element-wise, followed by activation for final output. The skip or shortcut connection, as described in residual blocks<sup>37</sup>, allows the network to connect the input of a layer directly to its output. This bypasses one or more layers within the neural network, enabling information propagation between distant layers. The connection is added to the output of a layer and then passes through an activation function, becoming the final output of the residual block. Skip connections help learn residual functions, which address input-output differences. Particularly effective for deep networks, they mitigate vanishing gradients during training. Also referred to as the identity connection, it enables the input to "skip" the residual block and directly connect to the output.

**Proposed CNN Model:** The proposed CNN model architecture is depicted in Figure 4, which encompasses an input layer designed to process input images of dimensions 224 x 224. The image is simultaneously passed through Residual Block and Wavelet Decomposition. The wavelet decomposition provides LL0, LH0, HL0, HH0 images. These images are passed through residual blocks for feature extraction. The LL0 is further decomposed in the 2nd stage to generate LL1, LH1, HL1 and HH1 decomposed features. The similar operation is repeated up to 4 stages of decomposition and outputs are concatenated at respective stages.

Let's represent the wavelet transform of the original image  $X$  as  $W$ . The wavelet transform of  $X$  can be represented as:

$$W(X) = (ca4, cd4, cd3, cd2, cd1) \quad \dots(3)$$

where  $W$  denotes the wavelet transform operator.

Where  $ca4$  is the approximation coefficient at fourth level, and  $cd4, cd3, cd2, cd1$  are the detail coefficients at fourth, third, second and first level respectively. To pass these features through a residual block, we can represent the residual block as a function  $F(x)$  that takes an input tensor  $x$  and applies a series of convolutional layers, activation functions, and skip connections to produce an output tensor.

Residual block output is given by:

$$F(x) = x + H(x) \quad \dots(4)$$

Where  $H(x)$  represents the residual connection, which is the convolutional layer output applied to the input  $x$ . To apply the residual block to the wavelet coefficients, we can use the following equation:

$$Y = F([ca4; cd4; cd3; cd2; cd1]) \quad \dots(5)$$

Where  $Y$  indicates 'output tensor' of the residual block.

$[ca4; cd4; cd3; cd2; cd1]$  denotes concatenation of  $ca4$  and all detail coefficients, and  $F$  is the function that applies the residual block to the concatenated coefficients.

Note that this equation represents a single instance of passing the wavelet coefficients through a residual block. To conduct a four-stage decomposition, this procedure should be iterated four times. The output of every residual block serves as input for the subsequent levels of the wavelet transform. Dense layer output for input  $x$  can be represented as,

$$h = \text{ReLU}(Wx + b) \quad \dots(6)$$

In the equation,  $W$  is weight matrix,  $b$  indicates bias vector, and Rectified Linear Unit activation function is "ReLU". The second dense layer acts as a classifier can be denoted as,

$$y = \text{softmax}(Vh + c) \quad \dots(7)$$

Where  $V$  represents the weight matrix,  $c$  stand for the bias vector. Softmax converts output to class probabilities. The final output predicts the class with the highest probability. Thus,

$$y = \text{softmax}(V(\text{ReLU}(Wx + b)) + c) \quad \dots(8)$$

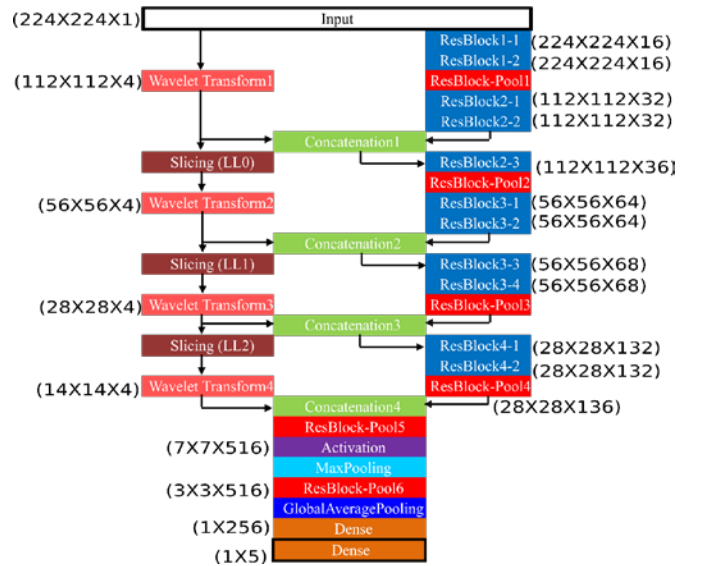


**Figure 4:** Proposed CNN model Architecture

## RESULTS AND DISCUSSION

Results of our study includes performance evaluation parameters which are listed in Table 2 and comparison of proposed module with existing different machine learning or deep learning techniques.

Interpretation of our findings, potential applications and the limitations of current approaches are noted here.

### K-Fold Analysis

Evaluation using Partitioning-based cross-validation<sup>38</sup> is a widely used technique in machine learning. In 10-fold cross-validation, the dataset is divided into 10 equal parts. The model is then trained and tested 10 times, each time using a different fold as the test set and the remaining folds for training. This allows for thorough evaluation, ensuring that each data point serves both for training and testing exactly once. The performance metrics from each fold are averaged to provide a robust estimate of the model's



effectiveness. This technique helps assess how well the model generalizes to unseen data and provides a reliable indication of its overall performance. [40]. Figure 5 shows 10-Fold analysis results.

**Table 2:** Performance Evaluation Parameters

Accuracy	$TP+TN/(TP+TN+FP+FN)$
Specificity	$TN/(TN+FP)$
Sensitivity or Recall	$TP/(TP+FN)$

Where TP = True Positive; TN = True Negative; FP = False Positive; FN = False Negative.

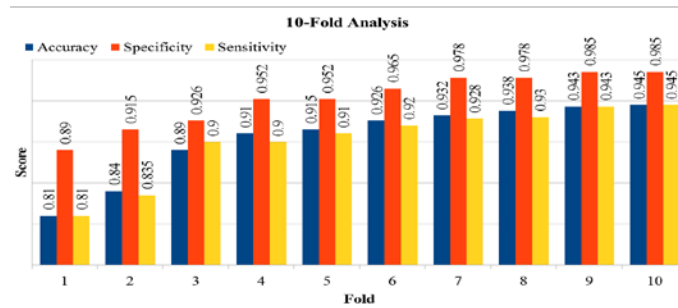


**Figure 5:** 10-Fold Analysis on Dataset3 for Three Way Classification

### Results with Different Wavelet Types

The study emphasizes the pivotal role of wavelet selection in medical image classification, notably for brain MRI. Different wavelets offer varied accuracy, with Daubechies-9 performing best due to its higher vanishing moments and superior frequency localization. This makes it particularly adept at detecting small features in medical images. Thus, our findings advocate for Daubechies-9 in such classification tasks. See Figure 6 for wavelet analysis.

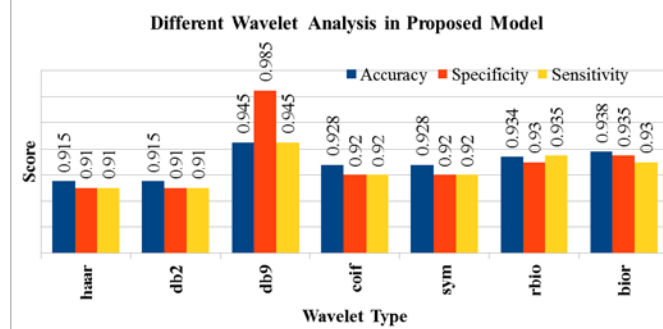
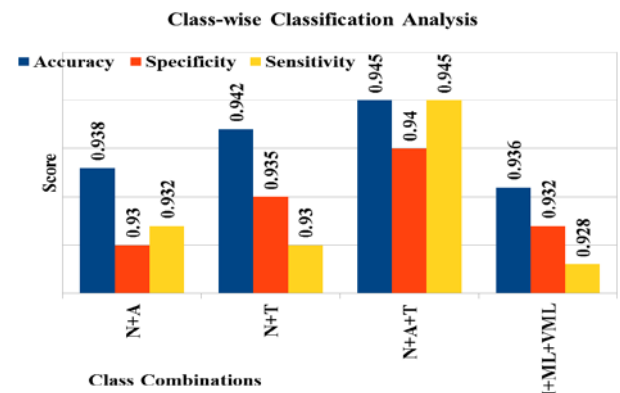


**Figure 6:** Analysis for different wavelet types

### Results of Class-wise classification Task

The classification of brain MRI images was assessed across binary, three-way, and four-way categories, aiming to improve disease diagnosis and treatment planning. Utilizing various datasets, including Alzheimer's and brain tumor data, the proposed CNN model, leveraging wavelet decomposition and Residual blocks, exhibited exceptional accuracy, specificity, and sensitivity. This versatile approach promises enhanced patient care. See Figure 7 for detailed performance analysis.



**Note:**  
N: Normal  
A: Alzheimer (ALL)  
T: Tumor  
M: Moderate Demented  
ML: Mild Demented  
VML: Very Mild Demented

**Figure 7:** Analysis for different Class-wise classification tasks

### Comparative Analysis with Existing edge cutting Models

When proposed model results compared with results of existing models such as VggNet-16, ResNet-50, ResNet-101, DenseNet-121, Xception, and MobileNet-V2, It is found that, proposed module is superior and effective

Existing models were chosen based on their popularity and performance in medical image classification tasks. For instance, ResNet-50, ResNet-101, and DenseNet-121 are renowned for their capacity to manage deeper layers and effectively learn intricate features. Meanwhile, VggNet-16 is a classic architecture extensively employed in image classification tasks. Additionally, Xception and MobileNet-V2 are recognized for their efficiency and accuracy in image classification tasks. The comparative study is shown in Figure 8.

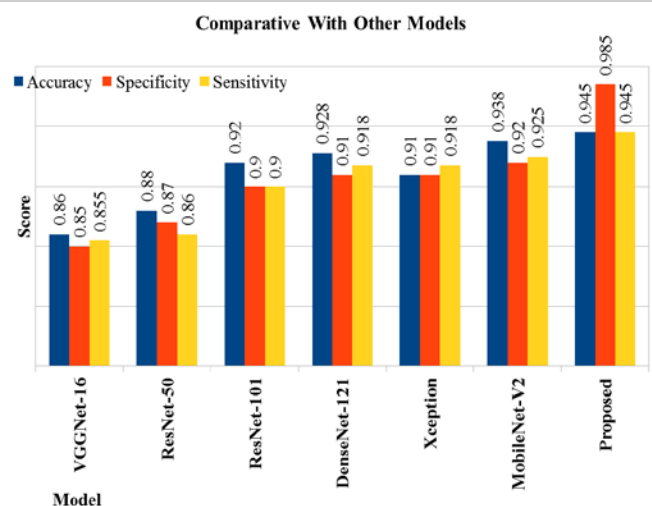


**Figure 8:** Comparison of proposed module with existing edge cutting models

The experimentation phase was conducted on a machine equipped with robust hardware specifications, featuring an Intel 11th generation i5 processor, 32 GB of RAM, and a GTX1660 graphics card with 6GB of memory. This setup provides sufficient computational power to manage the complex requirements of our model development and assessment processes. Required time for model Training is documented in Table 3.

**Table 3:** Required Time for Model Training

Model	Training Time	Average Inference Time
VGGNet-16	8 Hours	4 seconds
ResNet-50	6 Hours	5 seconds
ResNet-101	9 Hours	5 seconds
DenseNet-121	6.5 Hours	6 seconds
Xception	7 Hours	2.5 seconds
MobileNet-V2	5 Hours	2 seconds
Proposed	7.5 Hours	3.5 seconds

Several existing methods were reviewed for comparative analysis, each employing diverse techniques for multi-disease detection and multiclass classification. Kibriya et al.<sup>39</sup> utilized transfer learning with ResNet-18 and GoogleNet for feature extraction and SVM for classification. Nayak et al.<sup>40</sup> employed custom CNNs on MD1 and MD2 datasets, while Lampe et al.<sup>41</sup> used SVM for seven-way classification. Tandel et al.<sup>42</sup> utilized transfer learning to classify brain MR Images while Geneedy et al.<sup>43</sup> implemented classifier of Alzheimer's disease and healthy conditions using deep convolutional neural networks (CNNs) for the four-classes. Lin et al.<sup>22</sup> applied Linear Discriminant Analysis for AD detection and utilized an ensemble learning for tumor detection. Aurna et al.<sup>44</sup> utilized ensemble methods for four-class classification tasks, and Patil et al. utilized ensemble training for three-class brain tumor detection. Additionally, Khan et al.<sup>45</sup> employed transfer learning on the ADNI dataset for four-class Alzheimer's disease classification. These studies demonstrate the diversity of approaches and methodologies utilized in leveraging machine learning techniques to analyze brain MRI and diagnosing neurological disorders. Siddiqui et al.<sup>46</sup> used conventional machine learning with DWT features and PCA on the OASIS and Harvard datasets for multi-disease classification. Irmak et al.<sup>47</sup> developed a custom CNN strategy for multiclass brain disease classification. Table 4 presents a comprehensive comparative analysis of these methods alongside the proposed approach.

**Table 4:** Comparative Study

Method	Image Type Used	Number of Classes	Performance
CNN-SVM (ResNet18 and GoogleNet) <sup>39</sup>	MRI	4	Accuracy of 98%
Deep CNN method for MD1 and MD2 dataset <sup>[47]</sup>	MRI	5	accuracy 100.00% for MD 1 and 97.50% For MD-2 dataset

SVM classification <sup>41</sup>	MRI	7	71 and 95 % The binary SVM yielded high prediction accuracies
Transfer-learning-based CNN model <sup>42</sup>	MRI	5	Accuracies 100, 95.97, 96.65, 87.14, and 93.74%.
CNN <sup>43</sup>	MRI	4	Accuracy of 99.68%.
Linear Discriminant Analysis (LDA) and CNN <sup>22</sup>	Multi modal data	4	Accuracy 66.7% and 57.3% and F1-scores of 64.9% and 55.7%
Deep CNN <sup>48</sup>	MRI	4	accuracy of 99.13%
Ensemble Deep Convolutional Neural Network (EDCNN) <sup>44</sup>	MRI	3	Accuracy up to 97.77%.
Transfer learning base with tissue segmentation and pre-trained VGG 16, VGG 19 architecture <sup>45</sup>	MRI	4	accuracy of 97.89%
Several sub-models: like DWT, PCA, kNN, RF, LS-SVM <sup>46</sup> .	MRI	5	RF based classifier a 96% of accuracy and the performance of other classifiers varies 80% to 96%
Three different CNN models 1) Brain tumor detection (13 weighted layers)2) brain tumor types (25 weighted layers) 3) brain tumors into three grades (16 weighted layers) <sup>47</sup>	MRI	2,5,3	Accuracy for model 1, model2, model3 is 99.33%, 92.66%and 98.14% respectively
Proposed Model (Wavelet + Residual Block Based Model)	MRI	2,3,4	Accuracy of 93%, 94% and 93.8% for 2 classes, 3 classes and 4 classes respectively.

#### Clinical Validation:

A groundbreaking study delved into the clinical validation of Alzheimer's disease detection, utilizing a dataset comprised of 25 MRI images. The crux of this investigation lay in comparing the model's outcomes against evaluations conducted by seasoned medical experts. Upon meticulous analysis, the results spoke volumes. The model demonstrated an astonishing accuracy rate of 96%, accompanied by a specificity of 100%. In essence, this means the model accurately identified instances of Alzheimer's without misclassifying healthy subjects, ensuring a pristine level of precision in its diagnoses. Furthermore, with a sensitivity of 96%, the model exhibited a remarkable capacity to detect Alzheimer's cases among the subjects under scrutiny. Such findings underscored the model's immense potential in the realm of Alzheimer's

detection. The high accuracy, specificity, and sensitivity rates not only validated the model's efficacy but also hinted at its viability as a supplementary tool for medical professionals in diagnosing Alzheimer's disease. By leveraging advanced technology and machine learning algorithms, this study heralded a new era in Alzheimer's detection, offering a glimmer of hope for early intervention and improved patient care.

**Table 5:** Clinical Validation Results

Image Number	Medical Expert Opinion	Model's Outcome
1	Alzheimer's	Alzheimer's
2	Alzheimer's	Alzheimer's
3	Healthy	Healthy
4	Alzheimer's	Alzheimer's
5	Healthy	Healthy
6	Alzheimer's	Alzheimer's
7	Healthy	Healthy
8	Alzheimer's	Alzheimer's
9	Alzheimer's	Alzheimer's
10	Healthy	Healthy
11	Alzheimer's	Alzheimer's
12	Alzheimer's	Alzheimer's
13	Healthy	Healthy
14	Alzheimer's	Alzheimer's
15	Alzheimer's	Alzheimer's
16	Healthy	Healthy
17	Alzheimer's	Healthy
18	Healthy	Healthy
19	Healthy	Healthy
20	Alzheimer's	Alzheimer's
21	Alzheimer's	Alzheimer's
22	Healthy	Healthy
23	Alzheimer's	Alzheimer's
24	Alzheimer's	Alzheimer's
25	Healthy	Healthy

## Discussions

The potential contribution points of the proposed custom CNN model using residual block and 4 stage wavelet decomposition for analyzing Brain MRI images for multiple disease classification:

**Improved classification accuracy:** The model merges wavelet decomposition and residuals, capturing MRI's low- and high-level traits. Enhanced classification potential over separate techniques or CNNs. Also, model shows its good sensitivity for detection very mild conditions of AD.

**Reduced over fitting:** The use of residual blocks and discrete wavelet transform in the proposed model facilitates more relevant feature extraction this minimizes the chances of over fitting. Residual connections in the model directly access earlier information, making it easier to learn and less likely to just remember specific examples from the training data.

**Ability to handle multi-class classification:** The proposed model is designed, which handles multiple disease classification, which is a challenging problem in MRI image analysis. By incorporating

both wavelet decomposition and residual blocks, the model can capture the subtle differences between different disease classes and improve the classification performance.

**Interpretable features:** The use of wavelet decomposition can help extract interpretable features from the MRI images. The coefficients obtained from each level of the decomposition can give us an idea about the different spatial frequencies present in the images.

This model demonstrates its capability in extracting relevant features related to AD and shows superior classification performance compared to existing models. However, further analysis is needed to evaluate the model's performance when other disease classes are considered and to assess its robustness in detecting very mild AD conditions. Additionally, changes in brain volume due to other diseases may significantly impact the model's accuracy, highlighting the need for further evaluation with mixed diseased MRI images in the training and validation datasets.

## CONCLUSION

This article introduces an innovative CNN model designed for the categorization of brain Magnetic Resonance images into three categories: Alzheimer's disease, brain tumor, and normal conditions. The model leverages wavelet decomposition-based feature extraction and Residual blocks to facilitate efficient feature learning and classification. Upon evaluation using a dataset of brain MRI images, our model surpasses existing edge cutting models, achieving notable accuracy, specificity, and sensitivity scores of 0.945, 0.985, and 0.945 respectively. This work holds significant promise for enhancing an accuracy and efficiency of disease assessment and therapy strategizing based on brain MRI images. Accurate detection of multiple diseases from MRI images can prompt timely interventions, ultimately improving patient outcomes.

The experimental study entails selecting an appropriate wavelet type for feature extraction and evaluating the model's performance across binary, three, and four-class classification tasks. Results demonstrate the proposed model's excellent performance across all three scenarios, with Daubechies-9 (DB9) wavelet yielding the best classification performance. This underscores the importance of wavelet type selection for feature extraction and underscores the potential of the suggested model for diverse disease categorization tasks.

The suggested CNN model offers a robust approach for multi-class disease identification from brain MRI, boasting exceptional accuracy and efficiency. The utilization of wavelet decomposition-based feature extraction and Residual blocks facilitates efficient feature learning and disease classification. The implications of this model are substantial for improving disease diagnosis and treatment planning, ultimately leading to enhanced patient outcomes. Future research avenues may explore the model's applicability across other medical imaging modalities and disease categories, with further efforts focused on enhancing its performance.

## CONFLICT OF INTEREST STATEMENT

Authors declare that there is no known conflict of interest for this article.

## REFERENCES

1. J. Leszek, E. V. Mikhaylenko, D.M. Belousov, et al. The Links between Cardiovascular Diseases and Alzheimer's Disease. *Current Neuropharmacology* **2021**, 19 (2), 152.
2. A.P. Brady. Error and discrepancy in radiology: inevitable or avoidable? *Insights into Imaging* **2017**, 8 (1), 171.
3. H.P. Chan, R.K. Samala, L.M. Hadjiiski, C. Zhou. Deep Learning in Medical Image Analysis. *Advances in experimental medicine and biology* **2020**, 1213, 3.
4. G. Battineni, M.A. Hossain, N. Chintalapudi, et al. Improved Alzheimer's Disease Detection by MRI Using Multimodal Machine Learning Algorithms. *Diagnostics* **2021**, 11 (11).
5. Z. Zhang, G. Li, Y. Xu, X. Tang. Application of Artificial Intelligence in the MRI Classification Task of Human Brain Neurological and Psychiatric Diseases: A Scoping Review. *Diagnostics* **2021**, 11 (8).
6. A.S. Lundervold, A. Lundervold. An overview of deep learning in medical imaging focusing on MRI. *Zeitschrift für Medizinische Physik* **2019**, 29 (2), 102–127.
7. B. Menze, F. Isensee, R. Wiest, et al. Analyzing magnetic resonance imaging data from glioma patients using deep learning. *Computerized medical imaging and graphics : the official journal of the Computerized Medical Imaging Society* **2021**, 88, 101828.
8. N. Yamanakkanavar, J.Y. Choi, B. Lee. MRI Segmentation and Classification of Human Brain Using Deep Learning for Diagnosis of Alzheimer's Disease: A Survey. *Sensors (Basel, Switzerland)* **2020**, 20 (11), 1–31.
9. R. Wood, K. Bassett, V. Foerster, C. Spry, L. Tong. 1.5 Tesla Magnetic Resonance Imaging Scanners Compared with 3.0 Tesla Magnetic Resonance Imaging Scanners: Systematic Review of Clinical Effectiveness. *CADTH Technology Overviews* **2012**, 2 (2), e2201.
10. E. Tolosa, G. Wenning, W. Poewe. The diagnosis of Parkinson's disease. *The Lancet. Neurology* **2006**, 5 (1), 75–86.
11. A. Danielyan, H.A. Nasrallah. Neurological disorders in schizophrenia. *The Psychiatric clinics of North America* **2009**, 32 (4), 719–757.
12. J. Islam, Y. Zhang. Brain MRI analysis for Alzheimer's disease diagnosis using an ensemble system of deep convolutional neural networks. *Brain Informatics* **2018**, 5 (2), 1–14.
13. R. Fontana, M. Agostini, E. Murana, et al. Early hippocampal hyperexcitability in PS2APP mice: role of mutant PS2 and APP. *Neurobiology of aging* **2017**, 50, 64–76.
14. A.B.R. Shatte, D.M. Hutchinson, S.J. Teague. Machine learning in mental health: a scoping review of methods and applications. *Psychological medicine* **2019**, 49 (9), 1426–1448.
15. C. Salvatore, A. Cerasa, I. Castiglioni, et al. Machine learning on brain MRI data for differential diagnosis of Parkinson's disease and Progressive Supranuclear Palsy. *Journal of neuroscience methods* **2014**, 222, 230–237.
16. S.E. Sorour, A.A.A. El-Mageed, K.M. Albarrak, et al. Classification of Alzheimer's disease using MRI data based on Deep Learning Techniques. *Journal of King Saud University - Computer and Information Sciences* **2024**, 36 (2), 101940.
17. M. Mahmud, S. Vassanelli. Processing and analysis of multichannel extracellular neuronal signals: State-of-the-art and challenges. *Frontiers in Neuroscience* **2016**, 10 (JUN), 195309.
18. R.A. Poldrack, K.J. Gorgolewski, G. Varoquaux. Computational and Informatic Advances for Reproducible Data Analysis in Neuroimaging. <https://doi.org/10.1146/annurev-biodatasci-072018-021237> **2019**, 2, 119–138.
19. M. Mahmud, M.S. Kaiser, A. Hussain, S. Vassanelli. Applications of Deep Learning and Reinforcement Learning to Biological Data. *IEEE transactions on neural networks and learning systems* **2018**, 29 (6), 2063–2079.
20. M. Mahmud, M.S. Kaiser, T.M. McGinnity, A. Hussain. Deep Learning in Mining Biological Data. *Cognitive Computation* **2021**, 13 (1), 1–33.
21. A. Basher, B.C. Kim, K.H. Lee, H.Y. Jung. Automatic Localization and Discrete Volume Measurements of Hippocampi from MRI Data Using a Convolutional Neural Network. *IEEE Access* **2020**, 8, 91725–91739.
22. W. Lin, Q. Gao, M. Du, W. Chen, T. Tong. Multiclass diagnosis of stages of Alzheimer's disease using linear discriminant analysis scoring for multimodal data. *Computers in Biology and Medicine* **2021**, 134, 104478.
23. L. Zou, J. Zheng, C. Miao, M.J. McKeown, Z.J. Wang. 3D CNN Based Automatic Diagnosis of Attention Deficit Hyperactivity Disorder Using Functional and Structural MRI. *IEEE Access* **2017**, 5, 23626–23636.
24. C. Feng, A. Elazab, P. Yang, et al. Deep Learning Framework for Alzheimer's Disease Diagnosis via 3D-CNN and FSBi-LSTM. *IEEE Access* **2019**, 7, 63605–63618.
25. B. Jena, G.K. Nayak, S. Saxena. An empirical study of different machine learning techniques for brain tumor classification and subsequent segmentation using hybrid texture feature. *Machine Vision and Applications* **2022**, 33 (1), 1–16.
26. N.D. Cilia, T. D'Alessandro, C. De Stefano, F. Fontanella. Deep transfer learning algorithms applied to synthetic drawing images as a tool for supporting Alzheimer's disease prediction. *Machine Vision and Applications* **2022**, 33 (3), 1–17.
27. H. Alloui, M. Sadgal, A. Elfazziki. Utilization of a convolutional method for Alzheimer disease diagnosis. *Machine Vision and Applications* **2020**, 31 (4), 1–19.
28. T. Kaur, T.K. Gandhi. Deep convolutional neural networks with transfer learning for automated brain image classification. *Machine Vision and Applications* **2020**, 31 (3), 1–16.
29. K. Simonyan, A. Zisserman. Very Deep Convolutional Networks for Large-Scale Image Recognition. *3rd International Conference on Learning Representations, ICLR 2015 - Conference Track Proceedings* **2014**.
30. K. He, X. Zhang, S. Ren, J. Sun. Deep Residual Learning for Image Recognition. *Proceedings of the IEEE Computer Society Conference on Computer Vision and Pattern Recognition* **2015**, 2016-December, 770–778.
31. G. Huang, Z. Liu, L. Van Der Maaten, K.Q. Weinberger. Densely Connected Convolutional Networks. *Proceedings - 30th IEEE Conference on Computer Vision and Pattern Recognition, CVPR 2017* **2016**, 2017-January, 2261–2269.
32. F. Chollet. Xception: Deep Learning with Depthwise Separable Convolutions. *Proceedings - 30th IEEE Conference on Computer Vision and Pattern Recognition, CVPR 2017* **2016**, 2017-January, 1800–1807.
33. M. Sandler, A. Howard, M. Zhu, A. Zhmoginov, L.C. Chen. MobileNetV2: Inverted Residuals and Linear Bottlenecks. *Proceedings of the IEEE Computer Society Conference on Computer Vision and Pattern Recognition* **2018**, 4510–4520.
34. Alzheimer's Dataset ( 4 class of Images) | Kaggle <https://www.kaggle.com/datasets/tourist55/alzheimers-dataset-4-class-of-images> (accessed Apr 15, 2023).
35. D.F. Walnut. An Introduction to Wavelet Analysis; Applied and Numerical Harmonic Analysis; Birkhäuser Boston, Boston, MA, **2004**.
36. S. Basodi, C. Ji, H. Zhang, Y. Pan. Gradient amplification: An efficient way to train deep neural networks. *Big Data Mining and Analytics* **2020**, 3 (3), 196–207.
37. M. Mubashar, H. Ali, C. Grönlund, S. Azmat. R2U++: a multiscale recurrent residual U-Net with dense skip connections for medical image segmentation. *Neural Computing and Applications* **2022**, 34 (20), 17723–17739.
38. P. Refaellizadeh, L. Tang, H. Liu. Cross-Validation. *Encyclopedia of Database Systems* **2009**, 532–538.
39. H. Kibriya, M. Masood, M. Nawaz, R. Rafique, S. Rehman. Multiclass Brain Tumor Classification Using Convolutional Neural Network and Support Vector Machine. *Proceedings of the 2021 Mohammad Ali Jinnah University International Conference on Computing, MAJICC 2021* **2021**.
40. D.R. Nayak, R. Dash, B. Majhi. Automated diagnosis of multi-class brain abnormalities using MRI images: A deep convolutional neural network based method. *Pattern Recognition Letters* **2020**, 138, 385–391.
41. L. Lampe, H.J. Huppertz, S. Anderl-Straub, et al. Multiclass prediction of different dementia syndromes based on multi-centric volumetric MRI imaging. *NeuroImage: Clinical* **2023**, 37, 103320.
42. G.S. Tandel, A. Balestrieri, T. Jujaray, et al. Multiclass magnetic resonance imaging brain tumor classification using artificial intelligence paradigm. *Computers in Biology and Medicine* **2020**, 122, 103804.
43. M. EL-Geneedy, H.E.D. Moustafa, F. Khalifa, E. Abdelhalim. An MRI-based deep learning approach for accurate detection of Alzheimer's disease. *Alexandria Engineering Journal* **2023**, 63, 211–221.
44. N.F. Aurna, M.A. Yousuf, K.A. Taher, A.K.M. Azad, M.A. Moni. A classification of MRI brain tumor based on two stage feature level ensemble of deep CNN models. *Computers in Biology and Medicine* **2022**, 146, 105539.
45. R. Khan, S. Akbar, A. Mehmood, et al. A transfer learning approach for multiclass classification of Alzheimer's disease using MRI images. *Frontiers in Neuroscience* **2022**, 16.
46. M.F. Siddiqui, G. Mujtaba, A.W. Reza, L. Shuib. Multi-Class Disease Classification in Brain MRIs Using a Computer-Aided Diagnostic System. *Symmetry* **2017**, Vol. 9, Page 37 **2017**, 9 (3), 37.
47. E. Irmak. Multi-Classification of Brain Tumor MRI Images Using Deep Convolutional Neural Network with Fully Optimized Framework. *Iranian Journal of Science and Technology - Transactions of Electrical Engineering* **2021**, 45 (3), 1015–1036.
48. S. Patil, D. Kirange. Ensemble of Deep Learning Models for Brain Tumor Detection. *Procedia Computer Science* **2023**, 218, 2468–2479.